Ceramics

High-temperature mechanical behavior of partially sintered ceramics

Vojtěch Nečina[1], Sebastián E. Gass[2], Tereza Uhlířová[1], Mariano H. Talou[2,*] [iD],
M. Andrea Camerucci[2], and Analía G. Tomba Martinez[2]

[1] *Department of Glass and Ceramics, University of Chemistry and Technology, Prague (UCT Prague), Technická 5, 166 28 Prague 6, Czech Republic*

[2] *Institute of Research in Materials Science and Technology (INTEMA), CONICET/UNMdP, Av. Colón 10850, B7606BWV, Mar del Plata, Argentina*

ABSTRACT

The high-temperature mechanical behavior (elastic properties, fracture strength, and degree of irreversible deformation) of partially sintered alumina and zirconia ceramics with different porosities and degrees of sintering was evaluated by (static) three-point bending tests at 1100 °C, from which load–deflection curves were obtained. Furthermore, the elastic modulus obtained from these curves was compared to Young's modulus as measured via the impulse excitation technique. Bar-shaped specimens were prepared by uniaxial pressing and sintering at 1100, 1200, 1300 and 1400 °C for 2 h, and subsequently characterized via bulk density measurements, total porosity calculations and electron scanning microscopy analysis. The effects caused by progressive sintering and the occurrence of irreversible deformation due to the weak bonds (small sinter necks) between particles affected the values of the static elastic modulus, which resulted in values quite lower than those obtained by the impulse excitation technique. A very good correlation described with a power-law relationship was obtained between both type of modulus, dynamic and static one, in the whole range of sintering temperatures for the two evaluated porous ceramics. In particular, the very fine (nanocrystalline) grain size and the tendency to agglomerate of the zirconia powder facilitated the irreversible deformation by grain boundary sliding.

Introduction

Porous ceramic typically possess special combinations of characteristics and properties, such as low density, low thermal conductivity, high surface area, and high permeability, all of which determine their specific use in diverse technological fields involving high temperatures, e.g. in lightweight structures, thermal insulation, and filtration, to name a few. Nevertheless, it is worth noting that the mechanical properties of these types of materials as well as their structural stability in service conditions are often key factors that must be also considered since they limit their practical use. Thus, there is an inherent compromise made between designing porous microstructures for optimal performance and an adequate mechanical performance at high temperature, which requires a deep understanding of the relationship between the high-temperature mechanical behaviour and the characteristics of the developed microstructures.

A variety of processing routes can be employed to prepare different types of porous ceramics materials. Some of them are based on the use of templates or pore-forming agents, while others employ direct foaming techniques. Partial sintering is another way to obtain porous ceramics, either alone or in combination with other processes [1–9]. Moreover, the feasibility of obtaining microstructures with hierarchical porosity by using these routes provides an additional advantage with regard to the possible uses of the porous material [5–9].

The presence of concave pores in partially sintered materials provides these materials with unique properties which cannot be achieved in any other way. In particular, the concave pore shape (or, more precisely, the concave surface curvature of the pore space between the convex grains connected by sinter necks) is responsible for the fact that parts of the material are not involved in the load bearing, and consequently, reduces stiffness considerably [10]. This assertion indicates that partially sintered ceramics are much more "flexible" than their iso-porous counterparts with convex pores or cellular microstructures [11]. Several studies have focused on the elastic properties of partially sintered ceramics, especially the dependence of Young's modulus on porosity and temperature, from the point of view of the material's behavior as well as how sintering

evolves [1, 2, 8, 9, 11–13]. This is the case of porous alumina and zirconia, which are well-known structural ceramics suitable for high-temperature applications that require porous bodies (high-temperature thermal insulation and electrical furnace linings, lightweight kiln furniture, molten-metal filters, catalyst supports etc.). Now, studies carried out for partially sintered alumina ceramics concluded that the Young's modulus determined by the impulse excitation technique (adiabatic measurement) turned out to be significantly below the Pabst-Gregorová exponential prediction [11] for convex pores, as expected for partially sintered materials [14, 15]. Surprisingly, however, the dependence of Young's modulus measured by the impulse excitation technique on porosity for partially sintered zirconia (based on tetragonal zirconia polycrystals stabilized with 3 mol% Y_2O_3) obeys the Pabst-Gregorová exponential prediction quite closely [13]. This surprising behavior was explained by the tendency of nanosized zirconia powder to agglomerate and to form inter-agglomerate pores with essentially convex shape [13].

In this work, a different approach to the study of the high temperature mechanical behavior of such partially sintered ceramics, based on alumina and zirconia, was carried out based on (static) three-point bending tests at high temperature. The material's stiffness was evaluated via the (isothermal) elastic modulus, as well as the fracture strength at high temperature and the deformation experienced by the specimens, both less-explored aspects of the mechanical behavior of these materials. The testing was performed at 1100 °C under isothermal conditions on specimens with different porosities and degrees of (partial) sintering achieved by firing in the range of 1100–1400 °C.

Experimental procedure

Commercially available granulated alumina (CT 3000 SDP, Almatis, Germany) and 3 mol% yttria-stabilized zirconia (TZ-3YB-E, Tosoh, Japan) high-purity powders were used in this study. The alumina is a sub-micron powder (median grain size 0.6 μm), whereas the zirconia is nanocrystalline (crystallite size around 40 nm).

Rectangular bar-shaped alumina and zirconia specimens (final dimensions approximately 50 mm in length, 6 mm in width and 5.4 mm in height) were

prepared via uniaxial pressing with a pressure of 200 and 50 MPa for 30 s, respectively, and firing at different temperatures (T_S) in air. The values of T_S were 1100, 1200, 1300, and 1400 °C for both types of ceramics. An electrical furnace (Classic, Czech Republic) was employed using a heating rate of 2 °C/min and a dwell time of 2 h at T_S.

The bulk density of both types of as-fired specimens was determined using the Archimedes method (immersion in water). The total porosity values were calculated from the bulk density and the theoretical density of alumina (4.0 g/cm^3) and tetragonal zirconia (6.1 g/cm^3), respectively.

Firstly, Young's modulus was measured at room temperature via the impulse excitation technique (E_{dyn}) according to the ASTM E1876-09 standard (Sonelastic, ATCP, Brazil). In addition, the specimens fired at the different T_S were mechanically tested in in three-point bending at 1100 °C; this temperature corresponds to the lowest sintering temperature used for firing. A servohydraulic testing machine (INSTRON model 8501, UK), an electrical furnace (SFL, UK), and a silicon carbide three-point holder (span: 30 mm) were employed for the tests. The specimens were heated at 5 °C/min up to 1100 °C and remained for 30 min at this temperature before load was applied. The tests were performed in duplicate.

Load–deflection curves were obtained from the bending tests assuming that the stiffness of the assembly formed by the loading system and the SiC holder was high enough such that the displacement of the actuator matched the bar's deflection. The mechanical strength of the bars (σ_F) was calculated using the following Eq. (1):

$$\sigma_F = \frac{3F_{max}L}{2bh^2} \tag{1}$$

with F_{max} being the maximum applied load (kN), L the span (mm), b the width (mm) and h the height (mm). The elastic modulus (E_{st}) was calculated using the following relationship (2):

$$E_{st} = \frac{3pL^3}{2bh^3} \tag{2}$$

where p is the slope of the secant line of the load–deflection curve at 0.1 mm.

The fracture surface of all materials was analyzed by SEM (Tescan, Lyra 3, Czech Republic). The mean grain size was determined using ImageJ (Fiji

distribution) [16] by measuring grain area and calculating area-equivalent diameter (for each sample, the analysis was performed on 52–173 objects).

Results and discussion

Typical load–deflection curves for alumina and zirconia specimens sintered at different temperatures (1100–1400 °C) and tested at 1100 °C are shown in Fig. 1. Values of mechanical parameters obtained from these curves (fracture strength and elastic modulus) are shown in Table 1 together with the dynamic Young's modulus determined at room temperature (E_{dyn-RT}) and the total porosity of the sintered specimens. The dynamic Young's modulus
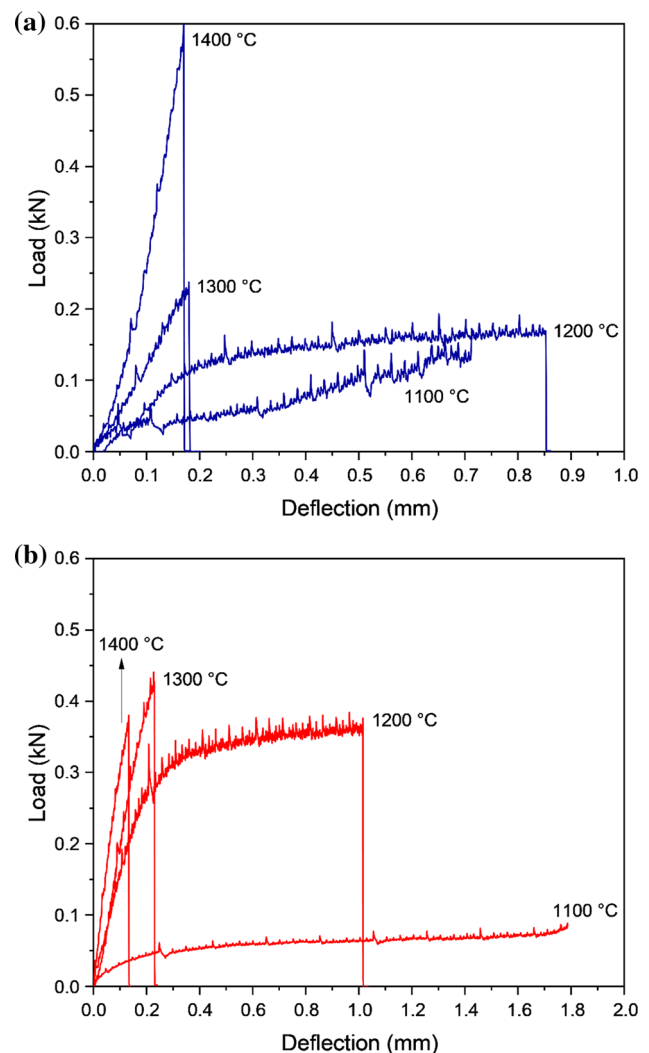

Figure 1 Typical load–deflection curves of alumina **a** and zirconia **b** specimens.

Table 1 Total porosity, mean grain size and mechanical parameters of alumina and zirconia specimens sintered between 1100 and 1400 °C, and mechanically tested at 1100 °C

Specimen	T_S (°C)	Total Porosity (%)	Mean grain size (µm)	$E_{\text{dyn-RT}}$ (GPa)	$E_{\text{dyn-1100}}$ (GPa)	$E_{\text{st-1100}}$ (GPa)	σ_F (MPa)
Alumina	1100	40.8 ± 0.7	0.2 ± 0.1	34 ± 2	–	3.2 ± 0.4	–
	1200	35.0 ± 0.1	0.3 ± 0.1	62 ± 3	40	4.5 ± 0.6	41 ± 2
	1300	30.0 ± 1.0	0.3 ± 0.1	106 ± 18	95	7.6 ± 0.6	62 ± 3
	1400	13.3 ± 0.7	0.4 ± 0.1	265 ± 9	190	30 ± 8	164 ± 55
Zirconia	1100	48.6 ± 0.3	0.15 ± 0.03	25 ± 1	25	2.6 ± 0.4	–
	1200	19.0 ± 0.1	0.22 ± 0.05	124 ± 1	100	20 ± 1	151 ± 1
	1300	5.0 ± 0.1	0.24 ± 0.08	193 ± 1	150	30 ± 4	210 ± 26
	1400	3.1 ± 0.1	0.28 ± 0.07	199 ± 5	165	41 ± 13	191 ± 6

T_S: sintering temperature

$E_{\text{dyn-RT}}$: dynamic Young's modulus at room temperature

$E_{\text{dyn-1100}}$: dynamic Young's modulus at 1100 °C

$E_{\text{st-1100}}$: static elastic modulus at 1100 °C

σ_F: mechanical strength

at 1100 °C ($E_{\text{dyn-1100}}$) was extracted from the previously determined curves of the Young's modulus as a function of the temperature obtained by testing each partially sintered material using the impulse excitation technique [11, 13].

Both materials exhibited similar mechanical behavior as the sintering temperature increased. For alumina and zirconia specimens sintered at the lower temperatures (1100 and 1200 °C), a marked non-linear behavior with large deflection was observed (Fig. 1). This behavior was more pronounced in the bars sintered at 1100 °C, which did not break but deformed irreversibly until the SiC holder prevented further deformation. The typical appearance of these specimens can be observed in Figs. 2a1 and b1, where the high propensity of such partially-sintered materials to deform irreversibly is evidenced. Zirconia specimens did not break at all but exhibited a permanent deflection (~ 1.6 mm), which represented around 30% of the bar's height; the deformation was much smaller for alumina (~ 0.6 mm). Bars sintered at 1200 °C exhibited catastrophic failure (Figs. 2a2 and b2); the permanent deflection decreased (to ~ 0.8 mm) for the zirconia samples and remained approximately unchanged (~ 0.6 mm) for the alumina samples. These results point out that, in addition to the increased reversible deformation (flexibility) characteristic of these particularly structured ceramics (with mainly concave pores) under load, they easily deform in a permanent manner (creep). The latter behavior will have important

consequence for the application of this type of porous ceramics. However, the authors did not find any previous reported data regarding the irreversible deformation of partially sintered alumina and zirconia materials.

After being treated at 1100 and 1200 °C, the materials had a high porosity (Table 1) associated with concave pores between the convex particles, which are connected only by small sinter necks, as shown in Figs. 3a1, a2, b1 and b2. These features are responsible for the mechanical behavior depicted above, as well as for the low values of $E_{\text{dyn-RT}}$ for alumina and zirconia bars sintered at 1100 and 1200 °C.

The values of the static elastic modulus at 1100 °C ($E_{\text{st-1100}}$) for samples treated at 1100 and 1200 °C increased along with the increase in T_S to quite a higher degree for zirconia specimens (~ 7.5 times) than for the alumina specimens (~ 1.5 times); this is mainly attributed to the greater reduction in the porosity of this material with respect to alumina (Table 1). In fact, nanocrystalline zirconia is commonly sintered between 1400 and 1500 °C [17], whereas submicron alumina is usually sintered between 1550 and 1600 °C [18] to achieve dense materials (> 99%).

On the other hand, the values of $E_{\text{st-1100}}$ shown in Table 1 for the specimens sintered at 1100 and 1200 °C are significantly lower than the corresponding values of $E_{\text{dyn-1100}}$: approximately 0.1 times lower for alumina and 0.1–0.2 for zirconia. These differences are in the range of 1–20 for dynamic to static
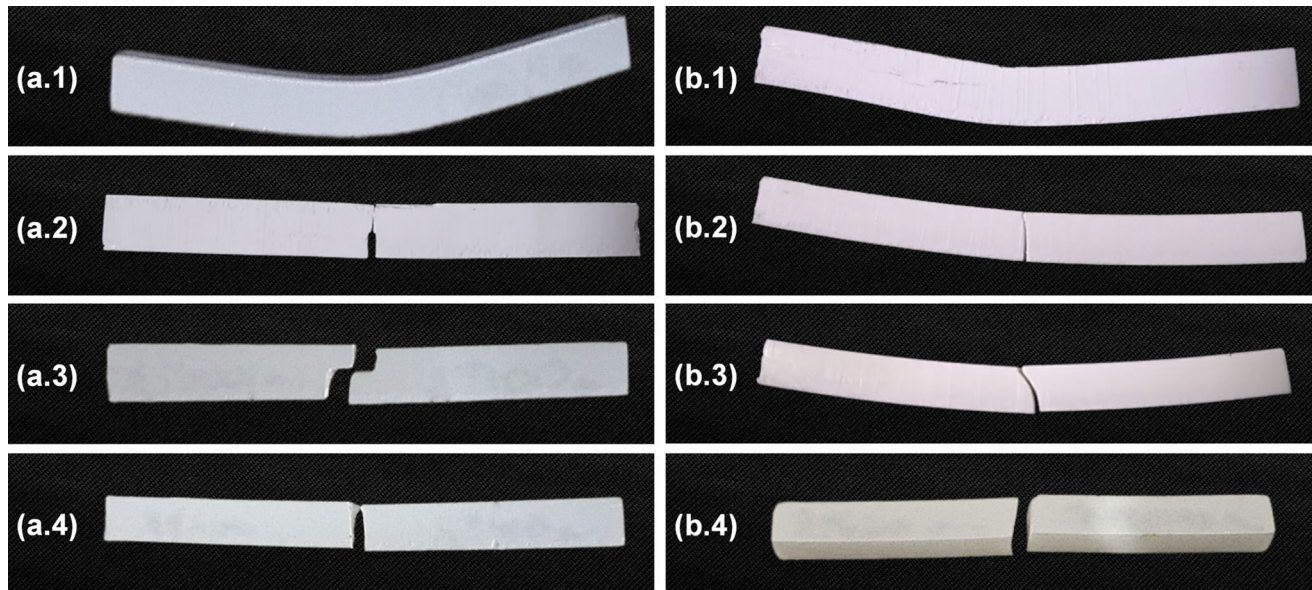
Figure 2 Images of alumina **a** and zirconia **b** specimens after mechanical testing at 1100 °C, sintered at T_S = 1100 °C (1), T_S = 1200 °C (2), T_S = 1300 °C (3) and T_S = 1400 °C (4).

Young's moduli ratio reported in the literature for similar types of materials like rocks [19]. There are several reasons for this difference. Firstly, the dynamic method provides adiabatic elastic constants, whereas the static method provides isothermal ones; therefore, the Young's modulus obtained from the former must always be higher. However, the difference between adiabatic and isothermal elastic constants should not be overestimated: actually, as long as the behavior is purely elastic, the relative difference between the two is usually not more than 1–2% [20]. On the other hand, as soon as anelastic effects come into play (which is typically the case at high temperatures, as evidenced e.g. by the increased damping in high-temperature impulse excitation measurements [13]), this difference increases dramatically. In particular, in static measurements any irreversible deformation is included in the measured deflection during the mechanical test, thus decreasing the slope of the load–deflection curve and the corresponding value of the elastic modulus to be determined from this curve. For example, Pabst et al. [20] reported greater differences between the isothermal and adiabatic Young's modulus of porous (convex pores) alumina and zirconia materials sintered at 1570 and 1490 °C, respectively, when the testing temperature was higher than ∼ 1000 °C and the mechanical behavior was no longer purely elastic. It has to be noted that in static measurements the elastic moduli themselves are affected by the anelastic effects at a much lower temperature than in dynamic measurements [20]. In the alumina and zirconia materials tested, the absence of strong bonding between particles when the sintering was performed at 1100 and 1200 °C led to even more irreversible deformation, as was observed in the tested specimens (Fig. 2). This behavior was a consequence of the grain boundary sliding, which is a typical process for fine-grained ceramics [21, 22] leading to a more significant deviation from the purely elastic behavior and a further reduction in $E_{st-1100}$ compared to $E_{dyn-1100}$ This deformation mechanism is supported by the intergranular fracture reported for very similar partially sintered alumina and zirconia materials [11, 23] and the fact that a similar mechanism is invoked for explaining the well-known superplasticity of dense nanocrystalline zirconia ceramics [24, 25]. The grain boundary sliding is easier to occur with smaller grain size and higher porosity [26] which is reflected by the lower irreversible deformation observed for higher T_S, as a result of lower porosity and larger grain size (see Table 1).

A notable change in the mechanical behavior at 1100 °C was observed when the alumina and zirconia bars were sintered at 1300 °C: the load–deflection curves are steeper, with quite lower deviation from the linear behavior and deformation at failure, and a significant increase in $E_{st-1100}$. These changes are in

Figure 3 SEM images of alumina **a** and zirconia **b** specimens sintered at $T_S = 1100$ °C (1), $T_S = 1200$ °C (2), $T_S = 1300$ °C (3) and $T_S = 1400$ °C (4).
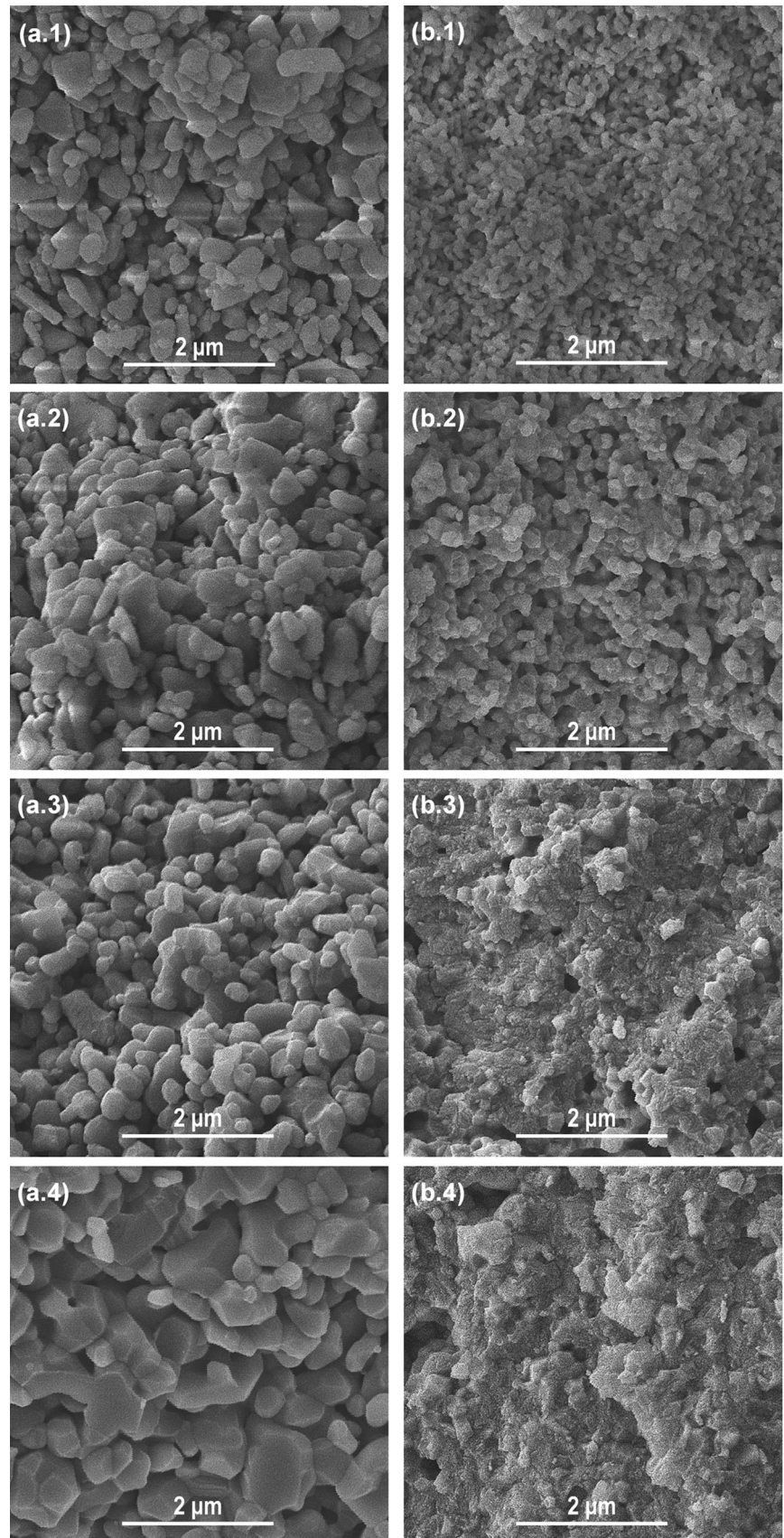
agreement with the more advanced sintering seen in the lower porosity (Table 1), and the growth of sinter necks and grain sizes (Fig. 3 and Table 1. Furthermore, as the convex particles change to polyhedral grains during sintering, the pore-space curvature tends to become more convex (see Fig. 4 for alumina materials sintered at the lowest and highest temperatures). All these microstructural changes obviously affect the values of E_{dyn-RT} and $E_{dyn-1100}$ as well,
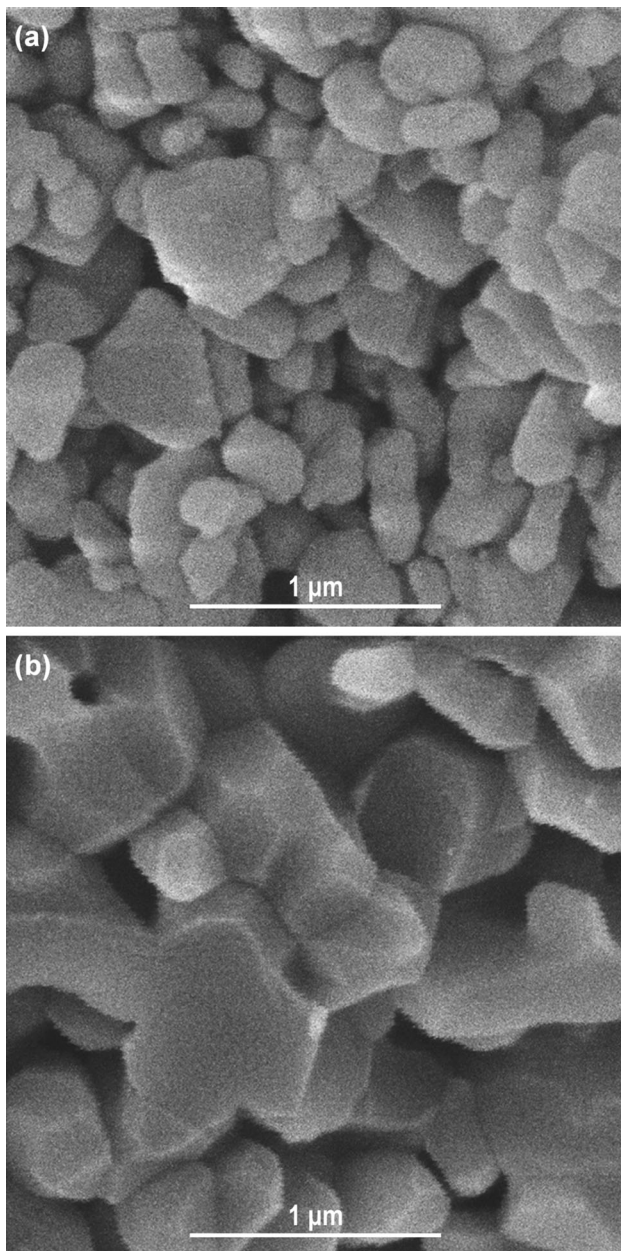

Figure 4 Magnified SEM images of alumina sintered at $T_S = 1100\ °C$ (**a**) and $T_S = 1400\ °C$ (**b**).

which also remained higher than the respective $E_{st-1100}$ for alumina and zirconia.

In addition, the load–deflection curves of alumina changed less than those of zirconia; for instance, the maximum load for alumina became two times higher when T_S changed from 1100 to 1300 °C, but it was seven times higher in the case of zirconia. This difference is mainly related to the higher densification achieved in the zirconia, manifested in its low residual porosity, in contrast to the sintering behavior of alumina fired at 1300 °C. Moreover, due to the tendency of the zirconia powder to agglomerate, a certain portion of convex pores is expected to be formed during pressing [13]. Considering this characteristic and the low porosity level, a very small portion of concave pores was probably still present in zirconia sintered at 1300 °C.

Irreversible deformation in the alumina and zirconia materials sintered at 1300 °C may have still occurred during the testing at 1100 °C, thus helping counteract the effect of sintering on $E_{st-1100}$. The presence of irreversible deformation during the mechanical testing was further confirmed by the slight curvature of tested bars (Figs. 2a3 and b3), with a permanent deflection smaller than 0.1 mm for both tested materials. The grain boundary sliding is considered to be the principal mechanism for such permanent deformation not only in zirconia, but also in the alumina since the sinter necks are not completely developed (Fig. 3a3) [11].

The load–deflection curves of specimens sintered at the highest temperature (1400 °C), displayed the same tendency observed when the specimens were sintered at 1300 °C. The reason for this analogous overall tendency is the same: a more advanced sintering process, as indicated by the reduced porosity measured for both materials sintered at 1400 °C (Table 1), and the further growth of sinter necks (Figs. 3a4, b4 and 4) [11].

However, closer inspection reveals that load–deflection curves of alumina sintered at 1400 °C were notably different from those displayed by the specimens treated at 1300 °C in terms of maximum load and the deformation at failure, along with the minimum difference between $E_{dyn-1100}$ and $E_{st-1100}$. Conversely, the load–deflection curves of the zirconia bars sintered at 1300 and 1400 °C are similar, as well as the maximum load and the $E_{st-1100}$ parameter. $E_{dyn-1100}$ shows just a slight increase (~ 1.1 times) compared to the value for bars treated at $T_S = 1300$ °C;

however, the value was higher ($\sim$ 1.5 times) when the specimens sintered at 1200 and 1300 °C are compared. Considering the small amount of residual porosity in zirconia, the degree of densification did not change significantly between 1300 and 1400 °C, which is the reason for the similarity in the mechanical behavior of zirconia specimens sintered at these low sintering temperatures. Conversely, the combination of a significant decrease in porosity and increase in grain size (Table 1), and the presence of well-developed sinter necks between particles generated a more noticeable difference in the mechanical response of the alumina specimens. In this context it has to be recalled that Young's modulus is around 400 GPa for fully dense alumina [11] but only 200–210 GPa for fully dense zirconia [13] and that the temperatures necessary for achieving full density are much higher for alumina than for zirconia (see above). Thus, the values of Young's modulus measured for zirconia sintered at 1400 °C are much closer to the asymptotic limit than for alumina sintered at the same temperature. It is worth noting that no permanent deformation was evident in the broken alumina bars sintered at 1400 °C (Fig. 2a4) and that the load–deflection curves are nearly linear in this case. Meanwhile, the load–deflection curves of the zirconia specimens exhibit a slight deviation from the linear behavior, which may be related to the small permanent deformation observed in the tested bars (Fig. 2b4), probably by a grain boundary sliding mechanism since the grain size (area-equivalent diameter) of this sample was only 0.28 μm.

In order to find a general relation between the elastic modulus measured by the impulse technique (E_{dyn}) and the mechanical test (E_{st}) at the same temperature (1100 °C), if such relationship actually exists, both parameters were plotted as shown in Fig. 5.
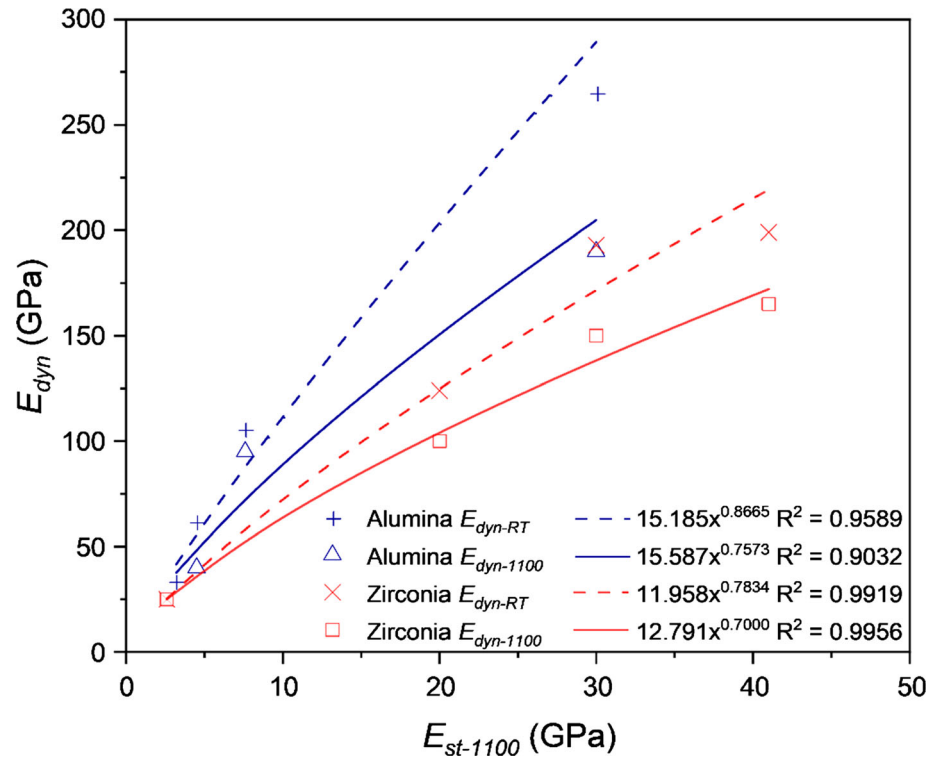
According to this figure, a good correlation was obtained, characterized by a non-linear dependency between $E_{dyn-1100}$ and $E_{st-1100}$. The best fitting (R^2 higher than 0.9) was obtained using a power-law for both partially sintered materials, similar to that reported for different type of rocks [27]. These are very interesting results, which support the use of such fitting curves to predict the static modulus using data from a non-destructive test. In this sense, values of E_{dyn-RT} were also plotted as a function of $E_{st-1100}$ in Fig. 5. It shows that, in spite of differences in the thermal conditions of both tests (room temperature

and 1100 °C), these modulus also exhibited a non-linear good correlation. In fact, the experimental values of E_{dyn-RT} and $E_{st-1100}$ data were also well fitted using a power-law with high R^2 for alumina ($\sim$ 0.90) and zirconia ($\sim$ 0.99) partially sintered materials. This means that the static modulus of such porous ceramics may be predicted in a reliable way using a parameter determined in a non-destructive and simple dynamic test at room temperature.

The specimens broken during the mechanical test, which corresponds to those sintered at 1200, 1300 and 1400 °C for both materials, exhibited the characteristics of a brittle fracture, as seen in the sudden drop in load observed in the curves in Fig. 1. The alumina and zirconia materials' fracture strength evolved similarly along with its stiffness, showing an increase when higher T_S were used, except for the fact that the strength values of the zirconia specimens sintered at 1300 and 1400 °C were very similar because their porosities were very similar. This behavior is a natural consequence of the sintering progress, which generated stronger bonding between particles and reduced porosity, since interconnected large pores (or the agglomeration of pores) have been identified as fracture origin in both types of materials [2, 28, 29].

Based on how the mechanical strength of both tested materials evolved with T_S, it appears that the alumina specimens could be more resistant when the same residual porosity possessed by zirconia sintered at 1400 °C is achieved. In fact, the fracture strength of the zirconia specimens was surely affected by the tendency of the very fine powder used for this study to agglomerate, and the relatively low load applied during pressing. As was previously reported [23], the different particles' packing generates defects in similar zirconia material, which negatively affects the strength of the bonds between grains. This parameter, designated as the 'interface bonding strength' was considered in this case to be a factor contributing to the mechanical behavior. According to the results obtained for zirconia sintered at 1300 and 1400 °C, the interface bonding strength did not change significantly in this thermal range since the degree of sintering approached an asymptotic limit in these temperature ranges, as was mentioned above.

Figure 5 Relationship between dynamic (E_{dyn}) and static (E_{st}) elastic modulus.

Legend:
- Alumina $E_{dyn\text{-}RT}$ — $15.185x^{0.8665}$ $R^2 = 0.9589$
- Alumina $E_{dyn\text{-}1100}$ — $15.587x^{0.7573}$ $R^2 = 0.9032$
- Zirconia $E_{dyn\text{-}RT}$ — $11.958x^{0.7834}$ $R^2 = 0.9919$
- Zirconia $E_{dyn\text{-}1100}$ — $12.791x^{0.7000}$ $R^2 = 0.9956$

Axes: E_{dyn} (GPa) vs $E_{st\text{-}1100}$ (GPa)

Conclusions

The high-temperature mechanical behavior of the alumina and zirconia ceramics partially sintered in the 1100–1400 °C range was studied using a conventional three-point bending at 1100 °C. Apart from the evolution of stiffness and mechanical strength of both materials due to sintering, mainly through the development of sinter necks and reduced porosity, permanent deformation, a less-explored aspect of the mechanical behavior of these materials could also be addressed. And, in addition to the flexibility related to the elastic behavior of materials with this special type of microstructure, the irreversible deformation that originated mainly in the weak bonds between particles is an important feature that will affect the practical application of these partially sintered ceramics as porous bodies. This irreversible deformation revealed itself by visual inspection of the specimens, i.e. the bars' aspect after the mechanical tests and the shape of the load–deflection curves, resulting in static Young's modulus values which were quite lower than those obtained via dynamic methods (such as the excitation impulse technique). As a very interesting and useful result, a very good correlation which can be described with a power-law relationship was obtained between both type of modulus in the whole range of sintering temperatures for partially sintered alumina and zirconia materials. Moreover, the very fine (nanocrystalline) grain size of the zirconia powder and the ensuing tendency to agglomerate affected the mechanical response of the resulting zirconia ceramics, making easier the irreversible deformation by grain boundary sliding.

Acknowledgements

Declarations

Conflicts of interest The authors declare that they have no conflict of interest.

References

[1] Lam DCC, Lange FF, Evans AG (1994) Mechanical properties of partially dense alumina produced from powder compacts. J Am Ceram Soc 77:2113–2117. https://doi.org/10.1111/j.1151-2916.1994.tb07105.x

[2] Hardy D, Green DJ (1995) Mechanical properties of a partially sintered alumina. J Eur Ceram Soc 15:769–775. https://doi.org/10.1016/0955-2219(95)00045-V

[3] Martin LP, Rosen M (2005) Correlation between surface area reduction and ultrasonic velocity in sintered zinc oxide powders. J Am Ceram Soc 80:839–846. https://doi.org/10.1111/j.1151-2916.1997.tb02912.x

[4] Nakata M, Suganuma K (2005) Effect of internal structure on thermal properties of alumina/aluminum composites fabricated by gelate-freezing and partial-sintering process, respectively. Mater Trans 46:130–135. https://doi.org/10.2320/matertrans.46.130

[5] Gregorová E, Uhlířová T, Pabst W et al (2018) Microstructure characterization of mullite foam by image analysis, mercury porosimetry and X-ray computed microtomography. Ceram Int 44:12315–12328. https://doi.org/10.1016/j.ceramint.2018.04.019

[6] Kocjan A, Shen Z (2013) Colloidal processing and partial sintering of high-performance porous zirconia nanoceramics with hierarchical heterogeneities. J Eur Ceram Soc 33:3165–3176. https://doi.org/10.1016/j.jeurceramsoc.2013.06.004

[7] Jean G, Sciamanna V, Demuynck M et al (2014) Macroporous ceramics: novel route using partial sintering of alumina-powder agglomerates obtained by spray-drying. Ceram Int 40:10197–10203. https://doi.org/10.1016/j.ceramint.2014.02.089

[8] Kalemtas A, Topates G, Özcoban H et al (2013) Mechanical characterization of highly porous β-Si$_3$N$_4$ ceramics fabricated via partial sintering & starch addition. J Eur Ceram Soc 33:1507–1515. https://doi.org/10.1016/j.jeurceramsoc.2012.10.036

[9] Gregorová E, Pabst W, Uhlířová T et al (2016) Processing, microstructure and elastic properties of mullite-based ceramic foams prepared by direct foaming with wheat flour. J Eur Ceram Soc 36:109–120. https://doi.org/10.1016/j.jeurceramsoc.2015.09.028

[10] Lurie SA, Solyaev YO, Rabinskiy LN et al (2018) Mechanical behavior of porous Si3N4 ceramics manufactured with 3D printing technology. J Mater Sci 53:4796–4805. https://doi.org/10.1007/s10853-017-1881-0

[11] Gregorová E, Pabst W, Nečina V et al (2019) Young's modulus evolution during heating, re-sintering and cooling of partially sintered alumina ceramics. J Eur Ceram Soc 39:1893–1899. https://doi.org/10.1016/j.jeurceramsoc.2019.01.005

[12] Liu X, Martin CL, Delette G, Bouvard D (2010) Elasticity and strength of partially sintered ceramics. J Mech Phys Solids 58:829–842. https://doi.org/10.1016/j.jmps.2010.04.007

[13] Gregorová E, Nečina V, Hříbalová S, Pabst W (2020) Temperature dependence of young's modulus and damping of partially sintered and dense zirconia ceramics. J Eur Ceram Soc 40:2063–2071. https://doi.org/10.1016/j.jeurceramsoc.2019.12.064

[14] Pabst W, Uhlířová T (2021) Benchmark polynomials for the porosity dependence of elastic moduli and conductivity of partially sintered ceramics. J Eur Ceram Soc 41:7967–7975. https://doi.org/10.1016/j.jeurceramsoc.2021.08.028

[15] Uhlířová T, Šimonová P, Pabst W (2022) Modeling of elastic properties and conductivity of partially sintered ceramics with duplex microstructure and different grain size ratio. J Eur Ceram Soc 42:2946–2956. https://doi.org/10.1016/j.jeurceramsoc.2022.01.053

[16] Schindelin J, Arganda-Carreras I, Frise E et al (2012) Fiji: an open-source platform for biological-image analysis. Nat Methods 9:676–682. https://doi.org/10.1038/nmeth.2019

[17] Amat NF, Muchtar A, Amril MS et al (2019) Effect of sintering temperature on the aging resistance and mechanical properties of monolithic zirconia. J Mater Res Technol 8:1092–1101. https://doi.org/10.1016/j.jmrt.2018.07.017

[18] Munro RG (2005) Evaluated material properties for a sintered α-alumina. J Am Ceram Soc 80:1919–1928. https://doi.org/10.1111/j.1151-2916.1997.tb03074.x

[19] Asef MR, Farrokhrouz M (2017) A semi-empirical relation between static and dynamic elastic modulus. J Pet Sci Eng 157:359–363. https://doi.org/10.1016/j.petrol.2017.06.055

[20] Pabst W, Gregorová E, Černý M (2013) Isothermal and adiabatic Young's moduli of alumina and zirconia ceramics at elevated temperatures. J Eur Ceram Soc 33:3085–3093. https://doi.org/10.1016/j.jeurceramsoc.2013.06.012

[21] Langdon TG (2006) Grain boundary sliding revisited: Developments in sliding over four decades. J Mater Sci 41:597–609. https://doi.org/10.1007/s10853-006-6476-0

[22] Ruano OA, Sherby OD (1995) High-temperature deformation mechanisms in ceramic materials. Plastic deformation of ceramics. Springer, US, pp 369–380

[23] Deng Z-Y, Yang J-F, Beppu Y et al (2002) Effect of agglomeration on mechanical properties of porous zirconia fabricated by partial sintering. J Am Ceram Soc 85:1961–1965. https://doi.org/10.1111/j.1151-2916.2002.tb00388.x

[24] Mayo MJ, Hague DC, Chen D-J (1993) Processing nanocrystalline ceramics for applications in superplasticity. Mater Sci Eng A 166:145–159. https://doi.org/10.1016/0921-5093(93)90318-9

[25] Yoshida H, Matsui K, Ikuhara Y (2012) Low-temperature superplasticity in nanocrystalline tetragonal zirconia polycrystal (TZP). J Am Ceram Soc 95:1701–1708. https://doi.org/10.1111/j.1551-2916.2012.05150.x

[26] Flacher O, Blandin JJ, Plucknett KP et al (1997) Effects of porosity on the superplastic properties of submicronic alumina-zirconia composites. Mater Sci Forum 243–245:411–416. https://doi.org/10.4028/www.scientific.net/MSF.243-245.411

[27] Davarpanah SM, Ván P, Vásárhelyi B (2020) Investigation of the relationship between dynamic and static deformation moduli of rocks. Geomech Geophys Geo-Energy Geo-Res 6:29. https://doi.org/10.1007/s40948-020-00155-z

[28] Adams JW, Ruh R, Mazdiyasni KS (2005) Young's modulus, flexural strength, and fracture of yttria-stabilized zirconia versus temperature. J Am Ceram Soc 80:903–908. https://doi.org/10.1111/j.1151-2916.1997.tb02920.x

[29] Flinn BD, Bordia RK, Zimmermann A, Rödel J (2000) Evolution of defect size and strength of porous alumina during sintering. J Eur Ceram Soc 20:2561–2568. https://doi.org/10.1016/S0955-2219(00)00133-3